Assessment of nozzle control strategies in weed spot spraying to reduce herbicide use and avoid under- or over-application

Sylvain Villette, Thibault Maillot, Jean-Philippe Guillemin, Jean-Paul Douzals

Citation

Villette, S., Maillot, T., Guillemin, J.-P., & Douzals, J.-P. (2022). Assessment of nozzle control strategies in weed spot spraying to reduce herbicide use and avoid under- or over-application. *Biosystems Engineering, 219*, 68-84. doi: https://doi.org/10.1016/j.biosystemseng.2022.04.012

Assessment of nozzle control strategies in weed spot spraying to reduce herbicide use and avoid under- or over-application.

S. Villette [1*], T. Maillot [1], J.P. Guillemin [1], J.P. Douzals [2]

[1] Agroécologie, INRAE, Institut Agro, Univ. Bourgogne, Univ. Bourgogne Franche-Comté, F-21000 Dijon, France
[2] UMR ITAP, INRAE, Montpellier SupAgro, Univ. Montpellier, 361 rue Jean-François Breton, F-34196 Montpellier cedex 05, France

[*] Corresponding author
E-mail address: sylvain.villette@agrosupdijon.fr

Abstract
Spot spraying is a method that can meet the objectives of reduced herbicide by maintaining a high level of weed control efficiency without lowering crop yield and harvest quality. Individual nozzle control systems show great potential for herbicide reduction. Nevertheless, this method of application also entails the risk of under-application on weed surfaces because of the lack of spray overlap and irregular dosing. Thus, nozzle control strategies need to be refined and assessed, regarding herbicide reduction and the ability to apply the prescribed dose on the target surfaces. Six control strategies were considered by activating complementary adjacent nozzles or increasing the flowrate of specific nozzles. Theoretical analyses and simulations were carried out to compare these strategies using three indicators. Considering a simplified description of the weed spatial distribution, a herbicide reduction indicator was expressed analytically for each strategy as a function of the weed coverage rate and patch width. For each strategy, numerical simulations were also carried out to compute under- and over-application indicators considering six weed coverage rates, eight patch widths and six different spray patterns. Graphs and charts were developed to provide convenient tools to help select the best technical approach for reducing chemical applied whilst keeping the prescribed dose on targets. In particular, a good compromise could consist of setting the weed detection width (associated with each nozzle) at twice the nozzle spacing and using triangular spray patterns combined with double spray overlaps.

Keywords
Precision agriculture; site specific weed management; spray pattern; theoretical approach; computer simulation.

Nomenclature

A	total field area, m²
A_S	total sprayed area, m²
$A_{SA>\beta}$	sprayed area exposed to over-application (relative to the threshold β), m²
A_W	total weed area, m²
a_w	patch area, m²
$A_{WA<\alpha}$	weed area exposed to under-application (relative to the threshold α), m²
a_Σ	neighbouring area associated with the segment Σ
$a_{\Sigma m}$	surface areas (with m from 1 to 6), m²
$CV(h)$	value of the coefficient of variation, at the boom height h, %
D_i	detection width associated with the i^{th} nozzle, m
$\mathrm{GA}i_{GA}$	geometric arrangements (with i_{GA} from 1 to 4)
h_s	boom height corresponding to the selected operating condition, m
k	number of weed patches
n_i	i^{th} nozzle of the spray boom
N_N	number of nozzles
$\mathrm{OC}i_{OC}$	operating conditions (with i_{OC} from 1 to 6)
$p(X)$	probability of X
p_Σ	probability of the detection segment Σ being above at least one patch
pi_p	probabilities (with i_p from 1 to 6)
Q_S	amount of herbicide used in the case of spot application, l
Q_T	amount of herbicide required for full broadcast application, l
q	nozzle flowrate, l s^{-1}
q_n	nozzle flowrate corresponding to the prescribed rate in broadcast application, l s^{-1}
q_x	nozzle flowrate relative to x, l m^{-1}
Sj	nozzle control strategies (with j from 1 to 6)
s_N	nozzle spacing, m
s_r	ellipse overlap area used to compute $a_{\Sigma 2}$, m²
$s_{r1/2}$	ellipse overlap area used to compute $a_{\Sigma 6}$, m²
T_Q	herbicide amount ratio
T_{QSj}	herbicide amount ratio when the nozzle control strategy is S_j, with j from 1 to 6
$T_{SA>\beta}$	ratio of sprayed area exposed to herbicide over-application (relative to the threshold β)
T_w	weed coverage rate
$T_{WA<\alpha}$	ratio of weed area exposed to herbicide under-application (relative to the threshold α)
u	semi-major axis of elliptical patches, m
v	semi-minor axis of elliptical patches, m
v_T	travel speed, m s^{-1}
W	working width associated with a nozzle, m
w_Σ	length of the detection segment Σ, m
w_w	weed patch width, m
x	spatial coordinate according to sprayer travel direction, m
X_w	number of patch centres located on the surface area a_w
X_Σ	number of patch centres located on the surface area a_Σ
y	spatial coordinate according to spray boom direction, m
α	percentage of the prescribed application rate defining the under-application threshold, %
β	percentage of the prescribed application rate defining the over-application threshold, %
δh	variation of the boom height, m
γ	coefficient of flowrate increase
λ	number of patch centres per unit area
$\mu_{\delta CVh}$	mean change of the CV value when the boom height fluctuates $\pm\delta h$, m
Σ	detection segment

Abbreviations

TSP	transverse spray pattern

CV coefficient of variation

1. Introduction

Weeds reduce crop yields and harvest quality because of their competition with crops, contamination of the harvest and their role in the transmission of pests (Oerke, 2006; Oerke & Dehne, 1997). For decades, the most popular approach for weed control has relied on uniform applications of herbicide across the entire field. This approach has environmental concerns in terms of water, air and soil contamination by pesticides as well as having public health issues. Regulatory frameworks have been designed and implemented to reduce the amount of pesticides used. For example, the French national action plan "Plan Ecophyto II+" (Ministère de la Transition écologique et solidaire, 2018) aims at reducing pesticides by 50% in 2025 compared to 2008. Thus, reducing herbicide use without lowering crop yields or harvest quality is a major challenge. In this context, spot spraying is a method of maintaining the use of certain herbicides whilst reducing the global amount used for weed control. The potential of this approach is supported by the spatial distribution of weeds since they often occur in patches within crop fields (Cousens & Croft, 2000; Dieleman & Mortensen, 1999; Mortensen, Johnson, & Young, 1993).

Various studies have addressed on/off spot spraying for post-emergence herbicide application and have studied performance in terms of reduction of the quantity of herbicide used. Field experiments have confirmed the potential of spot spraying but they have provided a wide variety of results (Castaldi, Pelosi, Pascucci, & Casa, 2017; Esau et al., 2018; Gutjahr, Sokefeld, & Gerhards, 2012) without possibility to relate precisely the herbicide reduction to characteristics of weed spatial distributions and sprayer spatial resolutions. Consequently, the use of models and numerical simulations appears as a convenient way to highlight how the herbicide use can be affected by the different parameters. Wallinga, Groeneveld, and Lotz (1998) considered one specific weed spatial distribution for an idealised patch sprayer applying herbicide in a circular zone around each weed. They estimated herbicide reductions of 15 %, 38%, 59% and 76% when the radius of the spraying surface was 4 m, 2 m, 1 m and 0.5 m respectively. Although this method is interesting, the results were obtained for only one specific weed spatial distribution. Moreover, the assumptions made were far from realistic since field sprayers produce rectangular deposit patterns that are not always centred on the target.

Recently, some studies have addressed the problem of selecting the appropriate boom section width for weed management by simulating more realistic spraying. The sprayed surfaces were then composed of rectangular deposit patterns whose widths depended on the number of activated boom sections and lengths depended on the distance travelled by the sprayer during activations. Franco, Pedersen, Papaharalampos, and Ørum (2017) simulated the spraying with section widths of 1 to 40 m. They performed simulations using two contrasting virtual weed maps built with circular patches of different diameters and two similar weed coverage rates (10 % and 10.9 %). They modelled the relative sprayed area as the sum of the weed coverage rate and a function of the boom section width. The potential use of the model was limited since it did not integrate any independent variable related to weed spatial distribution (such as patch size or weed aggregation degree). Moreover, the model implicitly assumed uniform distributions of herbicide under spray boom sections whatever the section width, so that the risk of under-application could not be studied. In addition, this model considered only one solution for section control. Villette, Maillot, Guillemin, and Douzals (2021) also used numerical simulations and modelled the herbicide use (with respect to a uniform whole-field application) as a function of the boom section width, weed patch size and coverage rate. This function was derived from simulations and successive regression analyses and not via a mathematical proof. Thus, there is a lack in the theoretical understanding of the relationship between the different parameters. Moreover, the expression of the herbicide use was established for only one solution of section control. Taking into account nozzle spray patterns, Villette et al. (2021) also addressed the problem of herbicide under-application owing to the lack of spray overlapping at the ends of each activate boom section when adjacent sections were switched off. They demonstrated that decreasing the active boom section width reduced herbicide use, but also increased the proportion of weed area exposed to herbicide under-application.

The above-mentioned studies only considered one simple solution for boom section or nozzle control. This consisted in switching on a boom section only when weeds were present under that section.

Unfortunately, regarding the application uniformity on target areas, this simple control strategy reaches its limit for small boom sections and especially in the case of independently controlled individual nozzles. Whilst studies have mainly focused on the analysis of herbicide quantity reduction, the ability to apply the prescribed dose to the target area requires more investigations. In the case of broadcast application, knowledge is available on how to reach the target dose on the sprayed area considering the even distribution of the product under the spray boom. The evenness of spray distribution results from the appropriate overlap of adjacent sprays obtained by a combination of nozzle type, nozzle spacing, pressure and boom height. However, in patch spraying systems, some nozzles or boom sections are switched off and uneven applications (in the transverse direction) can occur under activated nozzles owing to a lack of suitable adjacent spray overlap. The ensuing under-applications can then lead to weed-control failure and the emergence of herbicide-resistant weeds.

In another context, Holterman, van de Zande, and van Velde (2018) addressed the problem of maintaining a constant dose under a boom section of small width. They developed a model to design adequate nozzle set-ups on a sprayer boom optimized for bed-grown crops. In their spraying situation, the application is ideally uniform on the bed, whilst no spray was to be applied onto the paths between the beds. Since the bed width was constant, the width of the sprayed surfaces was also constant. Thus, the use of tilted edge blocks of nozzles at each end of the spray section was suggested to avoid a lack of spray overlapping at these section extremities. Unfortunately, in the case of herbicide spot spraying in conventional arable crops the width of weed patches and their location under the boom are random. They also continuously change along sprayer tracks in fields. Consequently, when each nozzle is controlled independently, the use of tilted nozzles at the extremity of a variable number of adjacent activated nozzles is not practical. Consequently the solutions suggested by Holterman et al. (2018) are not suitable for weed patch spraying in arable crops.

Considering the above-mentioned lacks or limits, the objective of the present study is to develop a model to help design and assess new nozzle control strategies for patch spraying systems considering not only the objective of herbicide reduction but also limiting under- or over-applications. The paper focuses on the case of spray booms equipped with nozzles controlled independently which offer the greatest potential of herbicide reduction. To circumvent cumbersome or unrealistic field experiments, the study considers a virtual sprayer and is carried out using theoretical analyses and computer simulations.

The paper has three main original contributions: i) the comparison of six nozzle control strategies based on the activation of adjacent nozzles or the increase of nozzle flowrate, ii) the establishment of analytical relationships to express herbicide reduction for each strategy using geometrical and probabilistic approaches, iii) the characterisation of under- and over-applications for each strategy using spraying simulations.

2. Materials and methods

The study considered a virtual spray boom equipped with independently-controlled nozzles. Six nozzle control strategies were developed to apply herbicide intermittently (section 2.1). The performance of each strategy was studied using three indicators defined to assess herbicide reductions as well as misapplications (section 2.2). To compare the different strategies, the weed spatial distribution was modelled by weed coverage rates and elliptical patch sizes (section 2.3). Using this spatial distribution, the analytical expression of a herbicide use ratio was established for each nozzle control strategy (section 2.4). Considering several nozzle spray patterns (section 2.5), under- and over-application indicators were computed using spraying simulations (section 2.6).

2.1. Nozzle control strategies

The nozzle control strategies consisted in activating adjacent nozzles or increasing the flowrate of certain nozzles to avoid or compensate the potential lack of transverse spray overlapping in spot spraying. Figure 1 illustrates the six different strategies studied in this paper. To help in describing the different strategies, some terms need to be defined. Firstly, the working width associated with a nozzle is defined as the width of the area centred vertically under the nozzle and which equals the nozzle spacing s_N (Fig. 1). Secondly, in order to describe the location of nozzles with respect to each other, the i^{th} nozzle of the boom is denoted by n_i.

Three control strategies, designated S1, S2 and S3, considered the use of the same flowrate q_n for each activated nozzle. These strategies differ by the activation (or not) of adjacent nozzles when weeds are present in the working width associated with a nozzle (Fig. 1).
In strategy S1, the nozzle n_i is activated when weeds are located within its working width. This is the simplest nozzle control and the one traditionally used in patch spraying studies (Franco et al., 2017; Gonzalez-de-Soto, Emmi, Perez-Ruiz, Aguera, & Gonzalez-de-Santos, 2016; Villette et al., 2021). Thus, in this work this common control is considered as the reference strategy.
Strategy S2 corresponds to the activation of the nozzle n_i when weeds are located within its working width and the activation of the adjacent nozzle (n_{i+1} or n_{i-1}) located on the side of the half working width associated with n_i where weeds are present.
Strategy S3 corresponds to the activation of the nozzle n_i when weeds are located within its working width and the activation of the two adjacent nozzles (n_{i+1} and n_{i-1}) whatever the location of the weed in the working width associated with n_i.
The strategies S1, S2 and S3 can also be defined by considering the detection width associated with each nozzle. This detection width is defined as the width of the area centred vertically under the nozzle and in which the presence of weeds triggers the activation of the nozzle (Fig. 2). Thus, the control strategies correspond to setting the detection width at s_N for S1, $2s_N$ for S2, and $3s_N$ for S3. In the example presented in Fig. 2, weeds are only located within half of the working width associated with the nozzle n_i. They are also located in the detection width associated with n_i in the case of S1, in the detection widths associated with n_i and n_{i+1} in the case of S2, and in the detection widths associated with n_{i-1}, n_i and n_{i+1} in the case of S3. Thus, the nozzle control rules for S1, S2 and S3 can be analysed in terms of activation of adjacent nozzles or in terms of detection width associated with the nozzles.
Three further strategies, designated S4, S5 and S6, were based on increasing the flowrate of certain nozzles, depending on the location of weeds with respect to the activated nozzles (Fig. 1). Thus, the flowrate q of certain switched-on nozzles is set at $(1+\gamma)q_n$ with $\gamma \geq 0$.
In the case of strategy S4, nozzles are activated when weeds are located within their working width and the flowrate is $(1+\gamma)q_n$ for isolated activated nozzles (*i.e.* switched-on nozzles without any adjacent activated nozzles). The flowrate is then maintained at q_n for non-isolated nozzles.
Strategies S5 and S6 focus on managing the flowrate of extremity nozzles. These extremity nozzles correspond to activated nozzles with another activated nozzle on one side and a non-activated nozzle on the other side. This is the case of the activated nozzle n_i if n_{i-1} is switched off and n_{i+1} switched on (or symmetrically).
In the case of strategy S5, nozzles are activated when weeds are located within their working width and the flowrate is increased to $(1+\gamma)q_n$ when weeds are located within the half working width on the side where there is no adjacent activated nozzle. The flowrate of other activated nozzles is maintained at q_n. Thus, the flowrate is increased for isolated nozzles and for certain extremity nozzles (depending on where weeds are located in their working widths).
In the case of strategy S6, nozzles are activated when weeds are located within their working width and the flowrate is increased to $(1+\gamma)q_n$ when there is no adjacent activated nozzle on one side. The flowrate of the other activated nozzles is maintained at q_n. Thus, the flowrate is increased for isolated activated nozzles and for all extremity nozzles.
The study assumed an instantaneous flow establishment or stop when a nozzle is switched on or off. Thus, an instantaneous herbicide application is considered under each activated nozzle, without any delay in sprayer response time or any smoothed herbicide rate transition along the travel direction.

2.2. Assessment indicators

Three dimensionless ratios were defined to study and compare the performances of the different nozzle control strategies. The herbicide use has been assessed through the ratio T_Q of the amount of herbicide used in the case of spot application Q_S divided by the amount of herbicide required for full broadcast application Q_T:

$$T_Q = \frac{Q_S}{Q_T} \tag{1}$$

Under-application of herbicide on weeds has been assessed through the ratio $T_{WA<\alpha}$ of the weed area $A_{WA<\alpha}$ (in m²) on which the application rate is lower than α % of the prescribed application rate divided by the total weed coverage area A_W (in m²) in the field:

$$T_{WA<\alpha} = \frac{A_{WA<\alpha}}{A_W} \tag{2}$$

Herbicide over-application has been assessed through the ratio $T_{SA>\beta}$ of the sprayed area $A_{SA>\beta}$ (in m²) on which the application rate is higher than β % of the prescribed application rate, divided by the total sprayed area A_S (in m²) actually exposed to herbicide in the field:

$$T_{SA>\beta} = \frac{A_{SA>\beta}}{A_S} \tag{3}$$

The values of these three assessment indicators are included in the bounded interval [0, 1].

2.3. Weed spatial distribution

To characterise and assess of the spraying strategies, virtual weed spatial distributions were designed by a set of elliptical weed patches randomly distributed in the field and oriented in the direction of cultivation operations. The choice of this theoretical shape was supported by the combination of natural dispersal processes and directional management practices (Dieleman & Mortensen, 1999; Paice, Day, Rew, & Howard, 1998) such as seed movements caused by soil tillage and crop harvesting (Barroso et al., 2006; Cousens & Croft, 2000). With this simplified representation, the weed spatial distribution was completely defined by the coverage rate T_w (*i.e.* proportion of weed area relative to the total area) and the semi-major and semi-minor axes (u and v) of the elliptical shapes. Nevertheless, random placements and patch overlapping provide a greater variety of patch shapes and sizes.

2.4. Analytical expression of the herbicide amount ratio

The above-mentioned model of weed spatial distribution was first used to establish the analytical expressions of the herbicide amount ratio T_Q by developing a geometrical and probabilistic approach.

2.4.1. Strategies S1, S2 and S3

Firstly, a plane was considered on which weed elliptical patches are distributed uniformly and independently. All the elliptical patches are oriented in the x-direction (corresponding to the sprayer travel direction) and have the same semi-major axis u and the same semi-minor axis v. The patch area is:

$$a_w = \pi u v \tag{4}$$

As shown in Fig. 3, a detection segment Σ was considered. It is oriented in the y-direction (corresponding to the boom direction) in the plane and its length is w_Σ. The detection segment Σ will be above one part of a patch if the centre of this patch is under a neighbouring surface associated with Σ (see Fig. 3). The area of this surface is:

$$a_\Sigma = 2uw_\Sigma + \pi u v \tag{5}$$

Let X_Σ be the number of weed patch centres located in the neighbouring area a_Σ associated with the segment Σ. The random variable X_Σ has a Poisson distribution with an intensity of λ patch centres per unit area. Thus, the probability of the boom section Σ being above k elliptical patches (at least partially) is the probability of observing k patch centres in the surface of area a_Σ. This probability is:

$$p(X_\Sigma = k) = \exp(-\lambda a_\Sigma)\frac{(\lambda a_\Sigma)^k}{k!} \tag{6}$$

Consequently, the probability of Σ being above at least one patch is:

$$p_\Sigma = p(X_\Sigma \neq 0) = 1 - p(X_\Sigma = 0) = 1 - \exp(-\lambda a_\Sigma) \tag{7}$$

Since λ is the mean number of patches per unit area, the expected weed coverage rate can also be established by considering the Poisson distribution of patches in the field. The probability of one point of the plane being covered by k weed elliptical patches is the probability of observing k patch centres on the area a_w. Considering the random variable X_w to count these occurrences, the probability is:

$$p(X_w = k) = \exp(-\lambda a_w)\frac{(\lambda a_w)^k}{k!} \quad (8)$$

Thus, the probability of a point of the plane being covered by at least one weed patch is:

$$p(X_w \neq 0) = 1 - p(X_w = 0) = 1 - \exp(-\lambda a_w) \quad (9)$$

The expected weed covered area is:

$$A_W = \int_A (1-\exp(-\lambda a_w))dS = A(1-\exp(-\lambda a_w)) \quad (10)$$

where A is the total field area.

Thus, the expected weed covered rate is:

$$T_W = \frac{A_W}{A} = 1-\exp(-\lambda a_w) \quad (11)$$

Expressing λ as a function of T_w using Eq. (11) and substituting in Eq. (7) yields:

$$p_\Sigma = 1-(1-T_w)^{\frac{a_\Sigma}{a_w}} \quad (12)$$

Thus, during the sprayer motion (along the x-direction), the expected amount of herbicide sprayed by one nozzle is:

$$Q_S = \int_L (1-(1-T_w)^{\frac{a_\Sigma}{a_w}})q_x dx = (1-(1-T_w)^{\frac{a_\Sigma}{a_w}})\int_L q_x dx \quad (13)$$

where: $q_x = q/v_T$ is the flowrate of herbicide sprayed by one nozzle relative to x, with v_T the travel speed, and L the travelled distance (along the x-direction).

In the case of a full broadcast application the expected amount of herbicide sprayed by one nozzle is:

$$Q_T = \int_L q_x dx \quad (14)$$

Thus, dividing Eq. (13) by Eq. (14) provides the expected sprayed amount ratio as follows:

$$T_Q = \frac{Q_S}{Q_T} = 1-(1-T_w)^{\frac{a_\Sigma}{a_w}} \quad (15)$$

with:

$$\frac{a_\Sigma}{a_w} = \frac{2uw_\Sigma + \pi uv}{\pi uv} = 1+\frac{2w_\Sigma}{\pi v} = 1+\frac{4w_\Sigma}{\pi w_w} \quad (16)$$

where w_w is the weed patch width ($w_w = 2v$).

The expression of T_Q is therefore directly related to the expression of the probability p_Σ (Eq. (12)). This relationship is in complete agreement with the one derived from simulations and successive regression analyses in Villette et al. (2021). Considering a boom section composed of N_N nozzles spaced of s_N, the detection width w_Σ associated with this boom section is $N_N \times s_N$.

In the case of single nozzles controlled independently, the detection width w_Σ associated with each nozzle is s_N (*i.e.* the nozzle spacing) for strategy S1, $2s_N$ for strategy S2 and $3s_N$ for strategy S3. Thus, Eq. (15) provides the expected sprayed amount ratios for the three nozzle control strategies considering:

$$\frac{a_\Sigma}{a_w} = 1+\frac{4s_N}{\pi w_w} \text{ for strategy S1} \quad (17)$$

$$\frac{a_\Sigma}{a_w} = 1+\frac{8s_N}{\pi w_w} \text{ for strategy S2} \quad (18)$$

$$\frac{a_\Sigma}{a_w} = 1 + \frac{12 s_N}{\pi w_w} \text{ for strategy S3} \quad (19)$$

2.4.2. Strategies S4, S5 and S6

In order to simplify the theoretical analysis of strategies based on flowrate increase, the herbicide application can be decomposed into an application following the strategy S1 and an additional application on certain areas (where the flow is increased by a proportion γ). The control strategy analysis leads to the identification of different geometric situations corresponding to different conditions of activation or non-activation of adjacent nozzles. Thus, in the vicinity of a detection segment Σ, four geometric arrangements (GA1 to GA4) were considered as depicted in Fig. 4. These lead to define six different surfaces $a_{\Sigma m}$ (with m from 1 to 6) in which weed patch centres must be present or absent (Fig. 4). The use of these parameters is detailed in the following subsections. Considering the previous analysis, the probability that at least one patch centre is located on a surface $a_{\Sigma m}$ is: $1-(1-T_w)^{\frac{a_{\Sigma m}}{a_w}}$, while the probability that no patch centre is located on the same surface is: $(1-T_w)^{\frac{a_{\Sigma m}}{a_w}}$. These properties are used to establish the expression of T_Q in the following sections. In order to simplify the mathematical reasoning, the expression of T_Q for strategy S5 is deduced from the expression obtained for S6. Thus, the analysis is first performed for strategy S6 and then for strategy S5.

2.4.2.1. Strategy S4

In the case of strategy S4, the herbicide application corresponds to S1 supplemented by an increase in the flowrate for activated nozzles in isolation (Fig. 1).

The probability p_1 of switching on a nozzle n_i in isolation (*i.e.* without any activated adjacent nozzle) is the probability that at least one patch centre is located on the surface $a_{\Sigma 2}$ and that there is no patch centre on surfaces $a_{\Sigma 1}$ associated with the adjacent nozzles n_{i+1} and n_{i-1} as depicted in Fig. 4 (GA2). This probability is as follows:

$$p_1 = \left(1-(1-T_w)^{\frac{a_{\Sigma 2}}{a_w}}\right)(1-T_w)^{\frac{a_{\Sigma 1}}{a_w}}(1-T_w)^{\frac{a_{\Sigma 1}}{a_w}} = \left(1-(1-T_w)^{\frac{a_{\Sigma 2}}{a_w}}\right)(1-T_w)^{\frac{2a_{\Sigma 1}}{a_w}} \quad (20)$$

where:

$$a_{\Sigma 1} = 2us_N + \pi uv \quad (21)$$

$$a_{\Sigma 2} = 2us_N - \pi uv + s_r \quad (22)$$

$$\begin{cases} s_r = 0 \text{ if } s_N \geq 2v \\ s_r = 4u\left(\frac{v}{2}\left(\frac{\pi}{2} - \arcsin\left(\frac{s_N}{2v}\right)\right) - \frac{s_N}{4v}\sqrt{v^2 - \left(\frac{s_N}{2}\right)^2}\right) \text{ if } s_N < 2v \end{cases} \quad (23)$$

Thus, considering Eqs. (15) and (20), the expected sprayed amount ratio in the case of strategy S4 is:

$$T_Q = \left(1-(1-T_w)^{\frac{a_{\Sigma 1}}{a_w}}\right) + \gamma\left(1-(1-T_w)^{\frac{a_{\Sigma 2}}{a_w}}\right)(1-T_w)^{\frac{2a_{\Sigma 1}}{a_w}} \quad (24)$$

2.4.2.2 Strategy S6

In the case of strategy S6, the application corresponds to that of strategy S4 supplemented by an increase in the flowrate for all extremity nozzles (Fig. 1).

The probability p_2 of having a non-activated nozzle n_{i-1} and an activated nozzle n_i is the probability of having at least one patch centre on the surface $a_{\Sigma 3}$ and the absence of a patch centre on the adjacent surface $a_{\Sigma 1}$ as depicted in Fig. 4 (GA1). This probability is as follows:

$$p_2 = (1-T_w)^{\frac{a_{\Sigma 1}}{a_w}} \left(1-(1-T_w)^{\frac{a_{\Sigma 3}}{a_w}} \right) \tag{25}$$

where:

$$a_{\Sigma 3} = 2us_N \tag{26}$$

Having a non-activated nozzle n_{i-1} and an activated nozzle n_i includes the case of nozzles activated in isolation. Thus, the probability p_3 of having a nozzle n_{i-1} non-activated, with nozzles n_i and at least n_{i+1} activated, requires excluding the situations of activated nozzles in isolation. Therefore, deducting Eq. (20) from Eq. (25) yields:

$$p_3 = (1-T_w)^{\frac{a_{\Sigma 1}}{a_w}} \left(1-(1-T_w)^{\frac{a_{\Sigma 3}}{a_w}} \right) - \left(1-(1-T_w)^{\frac{a_{\Sigma 2}}{a_w}} \right) (1-T_w)^{\frac{2a_{\Sigma 1}}{a_w}} \tag{27}$$

The probability of having a nozzle n_{i-1} not activated with nozzles n_i and at least n_{i+1} activated or the symmetrical situation (n_{i+1} not activated with n_i and at least n_{i-1} activated) is twice the previous probability p_3.

Thus, in the case of strategy S6, the expected sprayed amount ratio is deduced from Eqs. (24) and (27) as follows:

$$\begin{aligned} T_Q = & \left(1-(1-T_w)^{\frac{a_{\Sigma 1}}{a_w}} \right) + \gamma \left(1-(1-T_w)^{\frac{a_{\Sigma 2}}{a_w}} \right) (1-T_w)^{\frac{2a_{\Sigma 1}}{a_w}} \\ & +2\gamma \left((1-T_w)^{\frac{a_{\Sigma 1}}{a_w}} \left(1-(1-T_w)^{\frac{a_{\Sigma 3}}{a_w}} \right) - \left(1-(1-T_w)^{\frac{a_{\Sigma 2}}{a_w}} \right) (1-T_w)^{\frac{2a_{\Sigma 1}}{a_w}} \right) \end{aligned} \tag{28}$$

2.4.2.3 Strategy S5

In the case of strategy S5 (Fig. 1), the application corresponds to that of strategy S6 by removing the flow increase for the extremity nozzles for which weeds are only located in the half working width located on the side of activated nozzles.

The probability p_4 of having a nozzle n_{i-1} not activated and a nozzle n_i activated, with weeds lying on the half working width located on the side of activated nozzles, is the probability of having at least one patch centre on the surface $a_{\Sigma 5}$ and no patch centre on the adjacent surface $a_{\Sigma 4}$ as depicted in Fig. 4 (GA3).

$$p_4 = (1-T_w)^{\frac{a_{\Sigma 4}}{a_w}} \left(1-(1-T_w)^{\frac{a_{\Sigma 5}}{a_w}} \right) \tag{29}$$

where:

$$a_{\Sigma 4} = 3 \times s_N \times u + \pi \times u \times v \tag{30}$$

$$a_{\Sigma 5} = s_N \times u \tag{31}$$

The probability p_6 of having a nozzle n_{i-1} non-activated with the nozzles n_i and n_{i+1} activated requires excluding the situations of nozzles activated in isolation. The probability p_5 of having a nozzle n_i activated in isolation with weeds lying only within the half working width associated with n_i and following the geometrical arrangement GA4 (Fig. 4) is as follows:

$$p_5 = \left(1-(1-T_w)^{\frac{a_{\Sigma 6}}{a_w}} \right) (1-T_w)^{\frac{a_{\Sigma 4}}{a_w}} (1-T_w)^{\frac{a_{\Sigma 1}}{a_w}} \tag{32}$$

where:

$$a_{\Sigma 6} = us_N - \pi uv + s_{r1/2} \tag{33}$$

$$\begin{cases} s_{r1/2} = 0 \text{ if } s_N \geq 4v \\ S_{r1/2} = 4u\left(\frac{v}{2}\left(\frac{\pi}{2} - \arcsin\left(\frac{s_N}{4v}\right)\right) - \frac{s_N}{8v}\sqrt{v^2 - \left(\frac{s_N}{4}\right)^2}\right) \text{ if } s_N < 4v \end{cases} \quad (34)$$

Thus, deducting Eq. (32) from Eq. (29) provides the probability p_6 as follows:

$$p_6 = (1-T_w)^{\frac{a_{\Sigma 4}}{a_w}}\left(1-(1-T_w)^{\frac{a_{\Sigma 5}}{a_w}}\right) - \left(1-(1-T_w)^{\frac{a_{\Sigma 6}}{a_w}}\right)(1-T_w)^{\frac{a_{\Sigma 4}}{a_w}}(1-T_w)^{\frac{a_{\Sigma 1}}{a_w}} \quad (35)$$

The probability of having a nozzle n_{i-1} not activated with nozzles n_i and n_{i+1} activated (with weeds lying only in the half working width associated with n_i) or the symmetrical situation (n_{i+1} not activated with n_i and n_{i-1} activated) is twice the previous probability p_6.

Thus, in the case of strategy S5, the expected sprayed amount ratio is deduced from the one obtained for S6 by deducting $2\gamma p_6$ from Eq. (28) as follows:

$$\begin{aligned} T_Q &= \left(1-(1-T_w)^{\frac{a_{\Sigma 1}}{a_w}}\right) + \gamma\left(1-(1-T_w)^{\frac{a_{\Sigma 2}}{a_w}}\right)(1-T_w)^{\frac{2a_{\Sigma 1}}{a_w}} \\ &+2\gamma\left((1-T_w)^{\frac{a_{\Sigma 1}}{a_w}}\left(1-(1-T_w)^{\frac{a_{\Sigma 3}}{a_w}}\right) - \left(1-(1-T_w)^{\frac{a_{\Sigma 2}}{a_w}}\right)(1-T_w)^{\frac{2a_{\Sigma 1}}{a_w}}\right) \\ &-2\gamma\left((1-T_w)^{\frac{a_{\Sigma 4}}{a_w}}\left(1-(1-T_w)^{\frac{a_{\Sigma 5}}{a_w}}\right) - \left(1-(1-T_w)^{\frac{a_{\Sigma 6}}{a_w}}\right)(1-T_w)^{\frac{a_{\Sigma 4}}{a_w}}(1-T_w)^{\frac{a_{\Sigma 1}}{a_w}}\right) \end{aligned} \quad (36)$$

2.5. Single nozzle transverse spray patterns

While mathematical reasoning performed to establish the expression of T_Q did not require knowledge of nozzle spray patterns, they are required to assess the nozzle control strategies according to their ability to apply the right dosage on the target areas. Considering a spray boom equipped with nozzles spaced every 0.5 m (s_N), six operating conditions (OC1 to OC6) were studied. Thus, six transverse spray patterns (TSP) were chosen to model the spray deposit under single nozzles as presented in Fig. 5. Table 1 presents the main characteristics of the operating conditions selected for the study. The first operating condition (OC1) considered a theoretical triangular pattern with a spray width set to $2s_N$ (*i.e.* 1 m) at nozzle height of 0.5 m, providing a perfect even transverse distribution after overlapping. The other operating conditions considered more realistic spray patterns. These were derived from experimental measurements for a low-drift flat fan nozzle with a wide angle (CVI 110 02 Albuz Company, France), a low-drift flat fan nozzle with a narrow angle (IDK 90 02 Lechler Company, Germany) and from literature for an even flat fan narrow angle nozzle (TPE 80 03 Teejet Company, USA). For the CVI and IDK nozzles, reference TSP were measured at Julius Kühn-Institute, Braunschweig, Germany by Herbst (2019) by placing the nozzles at 0.6 m height, with a constant water pressure of 200 kPa and using a 25 mm channel spray patternator. For each type of nozzle, the pattern was computed as the average curve resulting from nine measurements corresponding to three repetitions with three different nozzles of the same series. For the TPE nozzle, the reference TSP was taken from Hassen, Sidik, and Sheriff (2013). The TSP at a specified boom height h was deduced from the reference TSP measured at the original experimental height h_0 following the method described by Mahalinga Iyer and Wills (1978). The relevant boom heights were selected for each kind of nozzle by computing the coefficient of variation (CV) of the spray deposit (ISO 5682-3, 2017) as a function of the boom height as described in Villette et al. (2021). Considering a broadcast application, for all selected boom heights (Tab. 1), CV values were lower than 7%, corresponding to a uniform spray in accordance with standards (ISO 16119-2, 2013). The sensitivity of the CV (*i.e.* spray uniformity) to the boom height was also estimated though the indicator defined as follows:

$$\mu_{\delta CVh} = \frac{\left|CV(h_s+\delta h) - CV(h_s)\right| + \left|CV(h_s-\delta h) - CV(h_s)\right|}{2} \quad (37)$$

where: $CV(h_s+\delta h)$, $CV(h_s)$ and $CV(h_s+\delta h)$ are the values of the CV when the boom height is set at $h_s+\delta h$, h_s and $h_s+\delta h$ respectively; h_s is the boom height corresponding to the selected operating condition; δh is the variation of the boom height (set at 0.05 m in this study).
The transverse spray patterns used in this study were all derived from static measurements carried out with conventional spray patternators free from any potential disturbance or displacement of the spray pattern related to travel speed, wind conditions or boom movement. Thus, this approach followed the standard methods used to assess the performance of horizontal boom sprayers. These spray patterns were therefore representative of practical herbicide application at low travel speeds (frequently required by real-time weed detection systems and autonomous sprayer robot) under calm conditions. In order to simplify the study and focus on the effect of the nozzle control strategy, the transverse spray patterns were assumed to be maintained irrespective of the nozzle flowrate.

2.6. Patch spraying simulations

To study misapplications, numerical patch spraying simulations were carried out using virtual weed maps. Using the weed spatial distribution presented in section 2.3, Villette et al. (2021) already demonstrated that the herbicide reduction ratio and the under-dosed weed area ratio only depended on the coverage rate and the patch width (irrespective of patch lengths). Consequently, weed maps were modelled with elliptical weed patches considering only one width to length ratio set at 0.5 and combining eight patch widths with six coverage rates. The patch widths w_w were set at 0.1, 0.25, 0.5, 1, 2, 4, 8 and 16 m; and the coverage rates T_w were set at 0.05, 0.10, 0.20, 0.30, 0.40 and 0.50. These provide 48 virtual weed spatial distributions. For each of these distributions, binary weed maps were built by placing full elliptical patches at random positions on 20 virtual fields (corresponding to 20 repetitions). Each virtual field was 72 m in width, 1000 m in length, and computed with a spatial resolution of 0.025×0.025 m/pixel. The field width corresponded to a sprayer pass with a working width of 24 m and two adjacent passes. Simulating three adjacent passes but analysing only the central pass avoided potential bias due to edge effects. Transverse spray patterns were also sampled every 0.025 m so that the sampling matched the weed map resolution.
Regarding the flowrate increase (for strategies S4, S5 and S6), the value of γ was set at 1 (*i.e.* 100% flow increase) so that the dosage was at least the prescribed dosage on the working width associated with an activated nozzle when it was isolated (*i.e.* from -0.25 m to +0.25 m on each side of the nozzle).
For $T_{WA<\alpha}$ and $T_{SA>\beta}$, the thresholds were set arbitrary at 85 % for α and 115 % for β so that both indicators equal 0 in the case of a full broadcast application, except for the operation condition OC5, for which the application rate exceeds the threshold of 115 % on 5 % of the sprayed area (see Fig. 5).
Overall, combining six coverage rates, eight patch widths, six operating conditions and six nozzle control strategies, 1,728 spraying simulations were computed. For each simulation, the indicator values were computed for 20 repetitions of virtual fields. Computing the cumulative average for each indicator, the convergence was checked by observing the maximum difference between the last value and the last five iteration values. For all of the 1,728 simulations, the maximum differences were lower than 0.0015 for $T_{WA<0.85}$, lower than 0.0020 for $T_{SA>1.15}$ and lower than 0.015 for T_Q.
The simulation algorithms were developed with the software MATLAB (2019).

3. Results

The assessment of the different nozzle control strategies was based on the results of the spraying simulations and on the use of the analytical relationships previously established.

3.1. Under-applications on weeds

Regarding strategy S1, for all operating conditions (OC1 to OC6), the proportion of weed area exposed to under-application $T_{WA<85\%}$ increased when patch width w_w and coverage rate T_w decreased (Fig. 6). This observation reflected the problem of the absence or lack of spray overlap when individual nozzles or a low number of adjacent nozzles are switched on over small weed patches widely dispersed in the field. In contrast, for weed patches wider than 2 m, $T_{WA<85\%}$ was lower than 0.10 for all the operating conditions.
Results obtained for the operating conditions OC2, OC4 and OC6 are similar and $T_{WA<85\%}$ reached high values for small patch size and coverage rate (higher than 0.43 for $w_w \leq 0.25$ m and $T_w \leq 0.10$). This

set of operating conditions corresponded to triple overlap settings (Fig. 5). The under-dosed surfaces were considerably less for OC1, OC3 and OC5 and decreased in this order. For example for $T_w = 0.10$ and $w_w = 0.25$ m, $T_{WA<85\%}$ was about 0.24, 0.15 and 0.04 respectively for OC1, OC3 and OC5. This set of operating conditions corresponded to double overlap settings.
Strategy S4 (Fig. 6) reduced $T_{WA<85\%}$ to less than 0.25 for all the situations and less than 0.10 when $w_w \geq 2$ m. In contrast to S1, depending on the width of the patch, $T_{WA<85\%}$ did not systematically decrease as a function of the coverage rate. For example, for patch widths of 0.1 and 0.25 m, the maximum value of $T_{WA<85\%}$ was obtained for coverage rates of 0.1 and 0.2 respectively. As well as S1, the operating conditions OC2, OC4 and OC6 yielded similar results and differed from OC1, OC3 and OC5. For example, for $T_w = 0.1$ and $w_w = 0.25$ m, $T_{WA<85\%}$ was about 0.15 for the first set of operating conditions whilst it was 0.07, 0.05 and 0.01 respectively for OC1, OC3 and OC5.
The maximal values reached by $T_{WA<85\%}$ for all studied situations are presented in Table 2. Simulation results obtained with strategies S2, S3, S5 and S6 demonstrated that these strategies are well suited to avoid under-application on weeds. Thus, $T_{WA<85\%}$ was zero when these strategies are combined with operating conditions OC1, OC3 and OC5. Moreover, $T_{WA<85\%}$ was lower than 0.023 for S2, lower than 0.007 for S5 and remained zero for S3 and S6 whatever the operating conditions.

3.2. Over-applications on sprayed areas
The strategies based on the activation of complementary adjacent nozzles (S1, S2, and S3) did not cause any over-application. Thus, $T_{SA>115\%}$ was zero for all weed spatial distributions and all operating conditions except for OC5 for which spray overlaps caused the dosage to locally exceed 115% of the prescribed rate (although $T_{SA>115\%}$ did not exceed 0.05 for OC5).
Over-applications ($T_{SA>115\%} > 0$) occured in the cases of strategies increasing the flowrate of some nozzles and the value of $T_{SA>115\%}$ logically increased successively from S4 to S5 and from S5 to S6 (Fig. 7). For S4, S5 and S6, the lowest values of $T_{SA>115\%}$ were obtained for the operating condition OC6. Higher values were obtained for OC1, OC3 and OC5 which were the best operating conditions regarding the reduction of under-application ($T_{WA<85\%}$). Thus, for S4, S5 and S6, OC5 was the best operating condition regarding $T_{WA<85\%}$ but the worst one regarding $T_{SA>115\%}$ which reached 0.34 for S4, 0.53 for S5 and 0.81 for S6 (when T_w was 0.05 and w_w was 0.5 or 1 m).
Over-applications were reduced for OC2, OC4 and OC6. For strategy S4 especially, $T_{SA>115\%}$ was zero for OC6 and limited to a maximum of 0.12 and 0.14 for OC2 and OC4 respectively. Surfaces exposed to over-applications increased in the cases of S5 and S6. The maximum values of $T_{SA>115\%}$ for OC2, OC4 and OC6 were respectively 0.26, 0.30 and 0.23 for S5, and 0.48, 0.53 and 0.46 for S6.
Except for strategy S4, strategies based on doubling the nozzle flowrate led to over-applications on a substantial part of the effective sprayed surface, especially in the case of small patches ($T_{SA>115\%}$ was more than 20% when weed patch widths were less than 2 m for strategy S5 and 4 m for strategy S6).

3.3. Herbicide amount ratio
The analytical expressions of T_Q were established mathematically. Numerical values of T_Q were also computed from simulations for certain weed coverage rates and patch sizes. Thus, the consistency of the results derived from simulations and from analytical expressions were checked beforehand. For the 1,728 simulations computed in this study, the linear regression between the numerical and analytical estimations of T_Q provided a coefficient of determination (R^2) greater than 0.999 whilst 96% of the differences between both estimations were lower than 0.015.
Thanks to the analytical expression of T_Q, the herbicide amount ratio was studied on a continuous domain of weed coverage rates (from 0 to 50%) and patch widths (from 0.01 to 32 m). To simplify the writing style, T_{QSj} was the herbicide amount ratio T_Q with the nozzle control strategy S*j*, where *j* was the strategy number (*i.e.* from 1 to 6).
In the case of strategy S1, Fig. 8 illustrates results deduced from Eq. (15) and (17), and represents T_{QS1} with respect to the weed coverage rate T_w for different weed patch widths. As expected, T_Q increased with T_w and when patch width decreased. It also shows that T_Q is very sensitive to low patch width values ($w_w \leq 2$ m) whilst differences are limited when patch widths are higher.
To compare the effects of the different control strategies for all weed spatial distributions, two-dimensional contour graphs were drawn (Fig. 9 to 11). They present colour scales and lines of equal

value representative of T_Q (Fig. 9) or differences in T_Q between two strategies (Fig. 10 and 11). The horizontal axis is plotted on a logarithmic scale to improve readability for all patch sizes.
Regarding the herbicide amount ratio T_Q, Fig. 9 summarises the performance of patch spraying in the case of strategy S1, with respect to weed spatial distributions (defined in terms of weed patch width w_w and coverage rate T_w). For example, for patches of 1 m in width, Fig. 9 indicates that the expected value of T_Q is approximately 0.3 when the coverage rate is 0.2 and 0.5 when the coverage rate is 0.35. Thus, Fig. 9 provides a quantification of T_Q for all weed spatial distributions in the case of strategy S1. Thanks to the analytical expressions of T_Q, such charts can be drawn for each nozzle control strategy.
With regard to the nozzle control rules defined for each strategy, the shift from S1 to S2 and S3 led to an increase of herbicide amount: $T_{QS1} \leq T_{QS2} \leq T_{QS3}$ for a given weed spatial distribution. Nevertheless, the increase in T_Q depends on the weed spatial distribution. To highlight the differences between strategies, Fig. 10 presents the level of deviation (absolute change) from the reference strategy S1. The figure quantifies the increase of herbicide amount ratio for S2 and S3 compared to S1 and shows how the weed spatial distribution (T_w and w_w) affects this increase. The figure also highlights the combination of coverage rates and patch widths for which T_Q is affected by strategy choice. In addition, it shows that differences tend towards zero when weed patches are wide enough or for very small patches when the coverage rate is high enough (greater than 25%). Overall, regarding all coverages rates and patch widths the maximum increase in T_Q for strategy S2 with respect to S1 is lower than 0.25.
Considering the strategies based on doubling the flowrate ($\gamma = 1$), the nozzle control rules led to: $T_{QS4} \leq T_{QS5} \leq T_{QS6}$. Curve comparisons deduced from analytical relationships show that T_{QS4}, T_{QS5} and T_{QS6} tend towards T_{QS1}, T_{QS2} and T_{QS3} respectively when the patch width increases. To refine the comparison, the differences for each strategy couple are shown in Fig. 11. Compared to differences observed between S1, S2 and S3, the differences observed in Fig. 11 are small since the maximal differences observed when patch width is higher than 0.1 m are 0.11, 0.04 and 0.08 for T_{QS4} - T_{QS1}, T_{QS5} - T_{QS2}, and T_{QS6} - T_{QS3} respectively. Moreover differences are all lower than 0.01 when patch width is higher than 2 m. For small patches (approximately lower than 0.5 m in width), particularities appear for S4 and S5 since the quantity of herbicide used relative to S2 and S3 respectively is higher or lower depending on the value of the coverage rate. This phenomenon is illustrated in Fig. 1 by observing zones B and C. Zone B shows a common situation when small patches are distributed at low coverage rates. The presence of small isolated patches leads to use more herbicide with S2 and S3 than with S5 and S6. In the case of higher coverage rates, narrow weed-free areas occur between weed patches as illustrated in zone C. In such situations, increasing the flowrate for two extremity nozzles requires more herbicide than adding one adjacent nozzle between two sets of switched-on nozzles. Thus, in zone C less herbicide is predicted with S2 and S3 than with S5 and S6.

4. Discussion

The implementation of spot spraying is a relevant solution to reduce the quantity of herbicide. Nevertheless, in the case of basic nozzle control strategies, the actual spray patterns of individual nozzles and the lack of spray overlap necessarily cause application rate variation on the surfaces exposed to the herbicide. Consequently, spot spraying can lead to injurious under dosing of herbicide on weeds, especially when weeds are distributed in small scattered patches. Thus, a substantial part of weed areas can be exposed to a sublethal dosage, leading to failure in weed-control, but also to select herbicide-resistant plants in weed populations. It has been shown that low herbicide use rate can lead to rapid evolution of non-target site-based resistance (Manalil, Busi, Renton, & Powles, 2011; Neve & Powles, 2005). To avoid increasing the soil weed-seed bank, evolving herbicide resistance and potential yield losses, herbicide doses must remain lethal and applications must be at the prescribed rate on all weed areas. Thus, $T_{WA<85\%}$ should be maintained at zero.
Therefore, the choice of reducing the weed surfaces exposed to an insufficient application rate and reducing the overall amount of herbicide requires compromise. To achieve the prescribed dose on the maximum target surface area, two types of approaches have been studied. They are based either on increasing the number of activated nozzles or increasing the flowrate of certain activated nozzles. Strategies based on increasing the flowrate (S4, S5 and S6) suffer from several drawbacks related to over-applications and potential technical difficulties in changing rapidly the flowrate of individual nozzles.

Except for one particular case (S4 combined with OC6), increasing the flowrate to reach at least the prescribed dosage on all the working width associated with a nozzle (where overlapping is lacking) leads to an over dosage of herbicide on one part of the sprayed surface.
From a legislative point of view, local over-application of herbicide is not considered problematic since the Regulation No 1107/2009 (European Council, 2009) defines the dosage of any plant protection product as the maximum dosage applied per hectare. Nevertheless, herbicide over-application may be problematic for some crops due to phytotoxicity (Holly, 1976). Selective herbicides are designed to kill target weeds and not damage the crop when applied at a specified application rate and especially in accordance with the maximum authorized dose. Thus, this maximum dose must not be exceeded and $T_{SA>115\%}$ should be zero or as low as possible.
In this paper, the coefficient of flowrate increase γ was set at 1, leading to double the flowrate for nozzles activated in isolation or at the edge of a sprayed area. Reducing this coefficient would reduce the over-application level but not eliminate it and it would not ensure a lethal dose of herbicide over the entire working width of each nozzle. Thus, choosing strategy S4, S5 or S6 and setting γ at a lower value does not appear as to be relevant.
From a technical point of view, the change of flowrate for only certain nozzles of the boom can also present some difficulties. A common way to modify the flowrate of nozzles is to change the hydraulic pressure but in a limited range. This solution is possible to use individually fed nozzles and not use nozzles mounted on a boom with a common feed which is the standard situation for most common boom sprayers. In this case, the use of multiple nozzle holders such as AmaSelect® (Amazone, Hasbergen, Germany) or Vario-Select® (Tecnoma, Epernay, France) can produce various flowrates at a constant pressure by selecting the correct nozzle size or by using several nozzles simultaneously. Alternative possibilities to increase the flowrate include using pressure increase and rely on variable orifice nozzles such as Turbo Drop Variable Rate® (GreenLeaf Technologies, Covington, USA) or VariTarget® tip (SprayTarget, Rosemount, USA) such as tested by Sharda, Fulton, and Taylor (2016).
To avoid the limitations of conventional flowrate control (imposed by the basic relationship between pressure, flowrate and droplet size), Giles and Comino (1990) demonstrated that the variation of flowrate (as required in S4, S5 or S6) can be carried using pulse width modulation (PWM) spray systems. However, Giles and Comino (1990) argued that the use of these systems influences the transverse distribution: as flowrate decreases, spray volume is more concentrated around the centre of the nozzle spray pattern. Recently, Butts, Luck, Fritz, Hoffmann, and Kruger (2019) studied the influence of pressure, nozzle type and PWM duty cycles. They showed that, across a wide range of nozzles and pressures, values of duty cycles at or above 40% have little impact on the uniformity of the spray patterns. The authors nevertheless recommend the use of non-venturi nozzles, because they are less impacted by duty cycle variations. Thus, in order to double the flowrate, varying the duty cycle from 50% to 100% would have limited effects on the spray pattern and spray droplet size spectrum. However, depending on operating conditions, these systems may have pressure drops affecting flow rate, droplet size and spray patterns (Fabula, Sharda, Kang, & Flippo, 2021).
The strategies based on activating adjacent nozzles (S2 and S3) appear as the more relevant to avoid both under-applications on weeds and over-application on crops. By ensuring proper spray pattern overlap on the working widths of the nozzles passing over weed patches, weeds are more reliably exposed to the prescribed dose of herbicide. Moreover, since spray characteristics of each individual nozzle do not change using these strategies, the quality of the spraying remains constant on weed areas. This quality is then equivalent to the one that would have been obtained in the case of broadcast applications. Nevertheless, the additional activation of adjacent nozzles leads to an increase in herbicide use compared to the reference strategy S1. The study quantified this increase and demonstrated that it depends on weed patch widths and coverage rates. The increase was found to be very small for large patches for which the changes in strategy only affect spraying at the edge of the patches. The spraying on these areas also represents a small proportion of the total herbicide amount used. In the case of very small patches, a coverage rate greater than 25% implies the frequent activation of adjacent nozzles due to the dispersion and the multitude of patches. This situation again leaves little area differentiating the application of the product according to strategies S1, S2 and S3.
This study not only demonstrated that refined nozzle control solutions can avoid under-dosage but it also provides a quantification of these solutions in terms of global herbicide use and potential savings. Thus, the analytical expressions and charts established in this study will help designers and users to

choose the solutions suited to their objectives with full background knowledge. Using a convenient spray pattern (*e.g.* OC3), the study demonstrated that strategy S2 avoid under- and over-applications ($T_{WA<85\%} = 0$ and $T_{SA>115\%} = 0$) with a limited increase of herbicide use compared to the reference nozzle control S1. Obtaining the relevant spray pattern means selecting the proper nozzle, liquid pressure and boom height. In the case of spot spraying, a double overlap of the spray deposit pattern leads to the more appropriate operating conditions. Double overlap provides the least under-applications in strategy S1 and no under-application in strategy S2. Triangular spray patterns such as OC1 and OC3 appear as good choices since they not only avoid under-application in strategy S2 but they are also robust to boom height fluctuations in terms of spraying quality (with the lowest values for $\mu_{\delta CVh}$ in Table 1). From this point of view, despite of good results to reduce under-applications, the use of even pattern nozzles (OC5) is limited by the high sensitivity of their spray quality to boom height (*i.e.* highest value for $\mu_{\delta CVh}$ in Table 1). Even flat-fan spray nozzles were designed for band spray applications to provide an even coverage from a single nozzle so it is not surprising that their transverse spray pattern is poorly suited in cases where spray pattern overlap is required.
In crosswind conditions, the strategies based on activating adjacent nozzles may also have an advantage over strategies based on increasing the flowrate of one nozzle. It has been demonstrated that the use of adjacent nozzles on a boom can have a positive influence on the lateral spray drift in a wind tunnel (Alheidary, Douzals, & Sinfort, 2020). The first spray pattern situated upwind will be obviously affected by the wind but it also plays a role in protecting the adjacent sprays downwind.
From a practical point of view, nozzle control based on activating adjacent nozzles (n_{i-1}, n_{i+1}), to improve overlapping spray deposition on weeds lying within the working width associated with the nozzle n_i, can be simply designed by increasing the detection width associated with each nozzle (Fig 2). Thus, the nozzle control corresponds to setting the detection width respectively at s_N for each nozzle in the case of S1, $2s_N$ in the case of S2, and $3s_N$ in the case of S3 (where s_N is the nozzle spacing). Thus, for example, analysing whether weeds are located on the either side of the detection width of nozzle n_i in strategy S2 will not be required. Thus, in practice the use of an approach based on the definition of detection widths is a simple but efficient way to address and implement nozzle control for map-based or real-time control systems.

5. Conclusion

The objective of weed spot spraying is to reduce the amount of herbicide used, but because of the lack of spray overlap, substantial proportions of the area of weed infestation can be exposed to under-dosage. Thus, refining nozzle controls is worthy of interest. For spot sprayers equipped with nozzles controlled independently, analytical relationships have been established to express the herbicide use as a function of the nozzle control strategy and the weed spatial distribution. Computer simulations have also been developed to study how the nozzle control strategy and the nozzle spray pattern affect under- or over-applications. The mathematical expressions and charts provided in this study are convenient tools to assist users and manufacturers in their technical choices to meet the challenge of reducing the global amount of herbicide use and maintain a high level of weed control efficiency. Results demonstrate that strategies based on activating complementary adjacent nozzles are better choices than those based on increasing the flowrate of a reduced number of nozzles. The control strategy designated S2 in this work appears as the best compromise and is obtained when the detection width associated with each nozzle is twice the nozzle spacing. Triangular spray patterns combined with double spray overlaps are also to be preferred. Although this work has been devoted specifically to weed control, it should have interest for any spot application with the objective of reducing the quantity of pesticide and maintaining treatment efficiency.

Acknowledgements

The work was supported by the higher national institute of agricultural science, food and environment (Institut Agro Dijon, France), and the French national research institute for agriculture, food, and environment (INRAE). The authors gratefully acknowledge Dr. A. Herbst, Julius Kühn-Institute (JKI), Braunschweig, Germany, for providing experimental data on transverse nozzle spray patterns.

References

Alheidary, M. H. R., Douzals, J. P., & Sinfort, C. (2020). An attempt to reduce spray drift in wind tunnel by substituting nozzles on the boom. *Agricultural Engineering International : The CIGR e-journal*, *22*(3), 86-94.
Barroso, J., Navarrete, L., Sanchez Del Arco, M. J., Fernandez-Quintanilla, C., Lutman, P. J. W., Perry, N. H., & Hull, R. I. (2006). Dispersal of *Avena fatua* and *Avena sterilis* patches by natural dissemination, soil tillage and combine harvesters. *Weed Research, 46*(2), 118-128. doi: https://doi.org/10.1111/j.1365-3180.2006.00500.x
Butts, T. R., Luck, J. D., Fritz, B. K., Hoffmann, W. C., & Kruger, G. R. (2019). Evaluation of spray pattern uniformity using three unique analyses as impacted by nozzle, pressure, and pulse-width modulation duty cycle. *Pest Management Science, 75*(7), 1875-1886. doi: https://doi.org/10.1002/ps.5352
Castaldi, F., Pelosi, F., Pascucci, S., & Casa, R. (2017). Assessing the potential of images from unmanned aerial vehicles (UAV) to support herbicide patch spraying in maize. *Precision Agriculture, 18*, 76-94. doi: https://doi.org/10.1007/s11119-016-9468-3
Cousens, R., & Croft, A. M. (2000). Weed populations and pathogens. *Weed Research, 40*(1), 63-82. doi: https://doi.org/10.1046/j.1365-3180.2000.00165.x
Dieleman, J., & Mortensen, D. (1999). Characterizing the spatial pattern of *Abutilon theophrasti* seedling patches. *Weed Research, 39*(6), 455-467. doi: https://doi.org/10.1046/j.1365-3180.1999.00160.x
Esau, T., Zaman, Q., Groulx, D., Farooque, A., Schumann, A., & Chang, Y. (2018). Machine vision smart sprayer for spot-application of agrochemical in wild blueberry fields. *Precision Agriculture, 19*(4), 770-788. doi: https://doi.org/10.1007/s11119-017-9557-y
European Council. (2009). Regulation (EC) No 1107/2009 of the European Parliament and of the Council of 21 October 2009 concerning the placing of plant protection products on the market and repealing Council Directives 79/117/EEC and 91/414/EEC. *Official Journal of the European Union*, 50 p.
Fabula, J., Sharda, A., Kang, Q., & Flippo, D. (2021). Nozzle Flow Rate, Pressure Drop, and Response Time of Pulse Width Modulation (PWM) Nozzle Control Systems. *Transactions of the ASABE, 64*(5), 1519-1532. doi: https://doi.org/10.13031/trans.14360
Franco, C., Pedersen, S. M., Papaharalampos, H., & Ørum, J. E. (2017). The value of precision for image-based decision support in weed management. *Precision Agriculture, 18*(3), 366-382. doi: https://doi.org/10.1007/s11119-017-9520-y
Giles, D. K., & Comino, J. A. (1990). Droplet size and spray pattern characteristics of an electronic flow controller for spray nozzles. *Journal of Agricultural Engineering Research, 47*, 249-267. doi: https://doi.org/10.1016/0021-8634(90)80045-V
Gonzalez-de-Soto, M., Emmi, L., Perez-Ruiz, M., Aguera, J., & Gonzalez-de-Santos, P. (2016). Autonomous systems for precise spraying – Evaluation of a robotised patch sprayer. *Biosystems Engineering, 146*, 165-182. doi: https://doi.org/10.1016/j.biosystemseng.2015.12.018
Gutjahr, C., Sokefeld, M., & Gerhards, R. (2012). Evaluation of two patch spraying systems in winter wheat and maize. *Weed Research, 52*(6), 510-519. doi: https://doi.org/10.1111/j.1365-3180.2012.00943.x
Hassen, N. S., Sidik, N. A. C., & Sheriff, J. M. (2013). Effect of nozzle type, angle and pressure on spray volumetric distribution of broadcasting and banding application. *Journal of Mechanical Engineering Research, 5*(4), 76-81. doi: https://doi.org/10.5897/JMER2013.0272
Herbst, A. (2019). [Personal communication: Results of the spray pattern measurements], Julius Kühn-Institut (JKI), Braunschweig, Germany.
Holly, K. (1976). Selectivity in relation to formulation and application methods. In L. J. Audus (Ed.), *Herbicides – Physiology, Biochemistry, Ecology* (Vol. II, pp. 249-275). London: Academic Press.
Holterman, H., van de Zande, J., & van Velde, P. (2018). Optimizing sprayer boom design for bed-grown crops. *International Advances in Pesticide Application, Aspects of Applied Biology, 137*, 123-130.
ISO 5682-3. (2017). Equipment for crop protection - Spraying equipment - Part 3: Test method to assess the performance of volume/area adjustment systems. International Organization for Standardization, Geneva, Switzerland.

ISO 16119-2. (2013). Agricultural and forestry machinery - Environmental requirements for sprayers - Part 2: Horizontal boom sprayers. International Organization for Standardization, Geneva, Switzerland.
Mahalinga Iyer, R., & Wills, B. M. D. (1978). Factors determining the design of tractor-mounted sprayer booms—sprayer nozzle characteristics. *Journal of Agricultural Engineering Research, 23*(1), 37-43. doi: https://doi.org/10.1016/0021-8634(78)90077-X
Manalil, S., Busi, R., Renton, M., & Powles, S. (2011). Rapid evolution of herbicide resistance by low herbicide dosages. *Weed Science, 59*(2), 210-217. doi: https://doi.org/10.1614/WS-D-10-00111.1
Matlab. (2019). Version 9.7. The MathWorks, Inc., Natick, Massachusetts, United States.
Ministère de la Transition écologique et solidaire. (2018). *Plan Ecophyto II+*. <http://www.consultation-ecophyto2plus.gouv.fr/IMG/pdf/plan-ecophyto_2_-_bat.pdf> Accessed 2022.09.10
Mortensen, D. A., Johnson, G. A., & Young, L. J. (1993). Weed distribution in agricultural fields. In P. C. Robert, R. H. Rust & W. E. Larson (Eds.), Proceedings of Soil Specific Crop Management (pp. 113-124). Madison, WI: American Society of Agronomy.
Neve, P., & Powles, S. (2005). High survival frequencies at low herbicide use rates in populations of *Lolium rigidum* result in rapid evolution of herbicide resistance. *Heredity, 95*(6), 485-492. doi: https://doi.org/10.1038/sj.hdy.6800751
Oerke, E. C. (2006). Crop losses to pests. *The Journal of Agricultural Science, 144*(1), 31-43. doi: https://doi.org/10.1017/S0021859605005708
Oerke, E. C., & Dehne, H. W. (1997). Global crop production and the efficacy of crop protection - current situation and future trends. *European Journal of Plant Pathology, 103*(3), 203-215. doi: https://doi.org/10.1023/A:1008602111248
Paice, M. E. R., Day, W., Rew, L. J., & Howard, A. (1998). A stochastic simulation model for evaluating the concept of patch spraying. Weed Research, 38(5), 373-388. doi: https://doi.org/10.1046/j.1365-3180.1998.00108.x
Sharda, A., Fulton, J. P., & Taylor, R. K. (2016). Performance of Variable-Orifice Nozzles for Liquid Fertilizer Applications. *Applied Engineering in Agriculture, 32*(3), 347-352. doi: https://doi.org/10.13031/aea.32.11428
Villette, S., Maillot, T., Guillemin, J. P., & Douzals, J. P. (2021). Simulation-aided study of herbicide patch spraying: Influence of spraying features and weed spatial distributions. *Computers and Electronics in Agriculture, 182*, 105981. doi: https://doi.org/10.1016/j.compag.2020.105981
Wallinga, Groeneveld, & Lotz. (1998). Measures that describe weed spatial patterns at different levels of resolution and their applications for patch spraying of weeds. *Weed Research, 38*(5), 351-359. doi: https://doi.org/10.1046/j.1365-3180.1998.00106.x

Figures

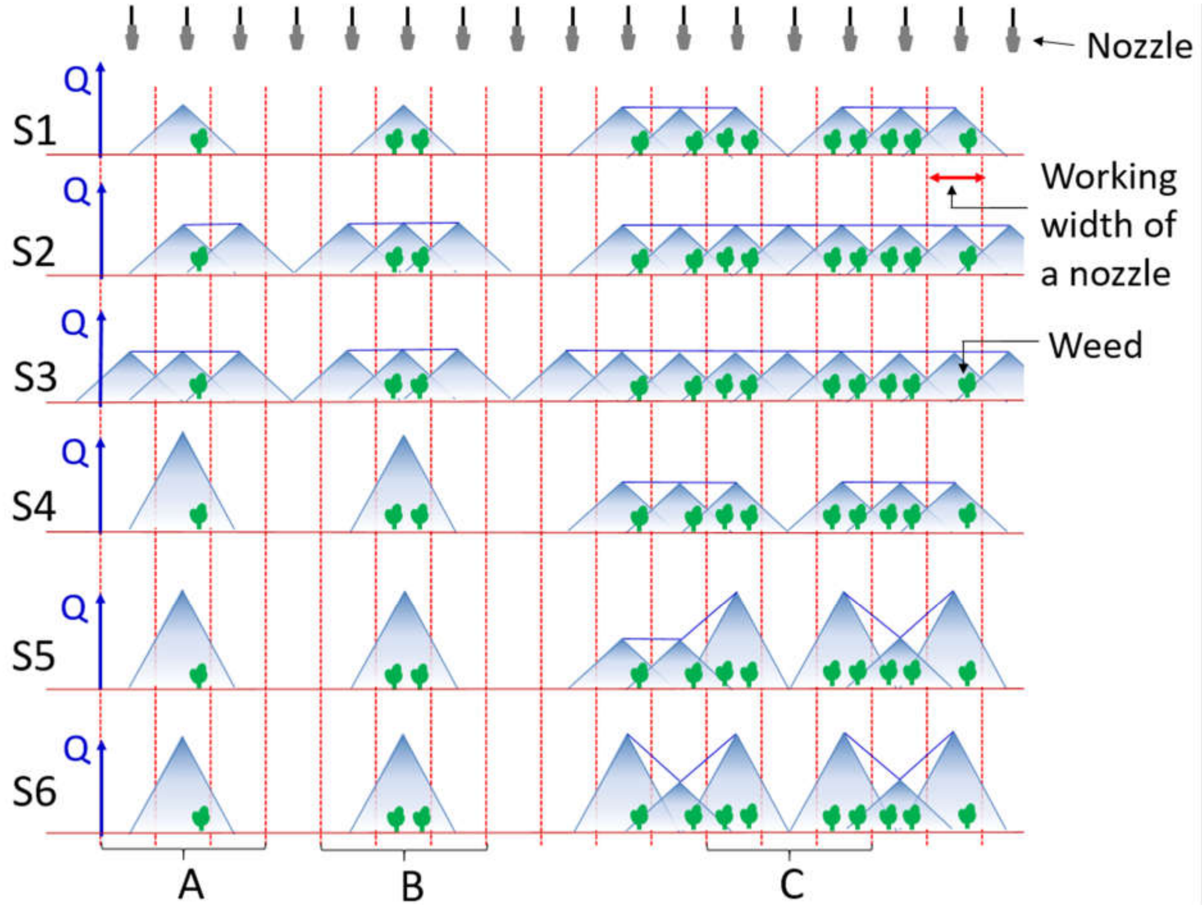

Fig. 1 - Illustration of the transverse amount Q of herbicide applied by each nozzle for different control strategies (S1 to S6) for the same example of weed locations, and in the case of a triangular transverse spray pattern. Three particular situations are highlighted: an isolated patch located on the half working width associated with a nozzle (area A), an isolated patch located on the whole working width associated with a nozzle (area B), a border area of two neighbouring patches (area C).

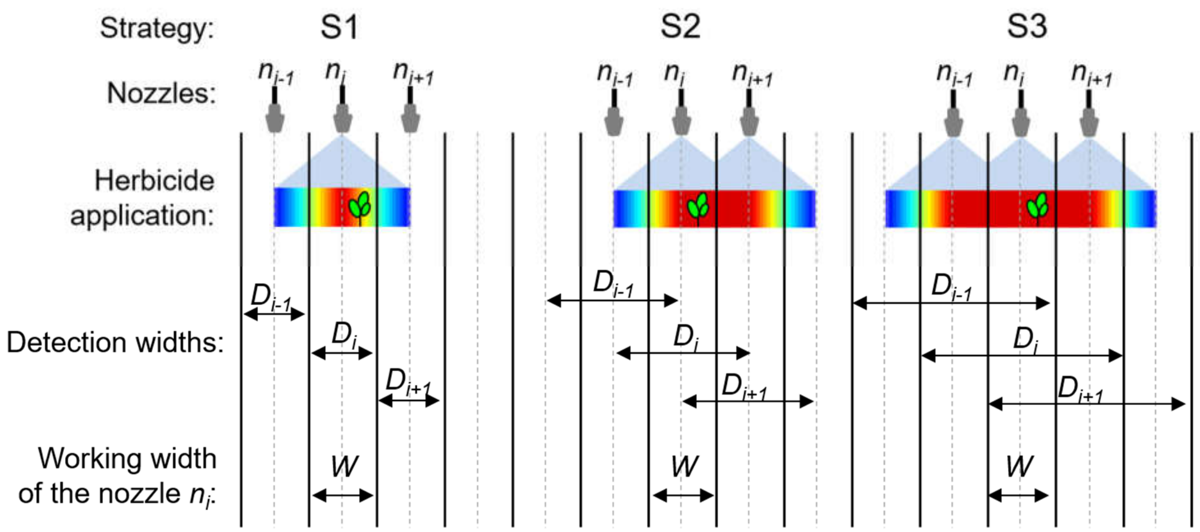

Fig. 2 - Illustration of the nozzle detection width defined for the three nozzle control strategies S1, S2 and S3. D_{i-1}, D_i and D_{i+1} are the detection widths associated with the nozzles n_{i-1}, n_i and n_{i+1}, while W is the working width.

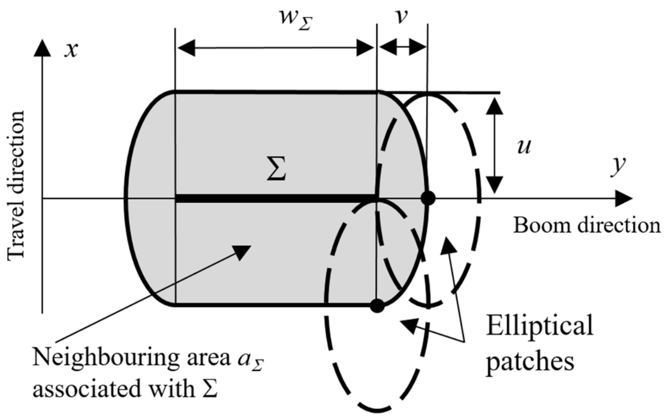

Fig. 3 - Top view of the neighbouring area a_Σ (in grey) on which are located the centres of all the elliptical patches covering the segment Σ (at least partially). w_Σ is the width of the detection segment Σ, u and v are respectively the semi-major and semi-minor axes of elliptical patches.

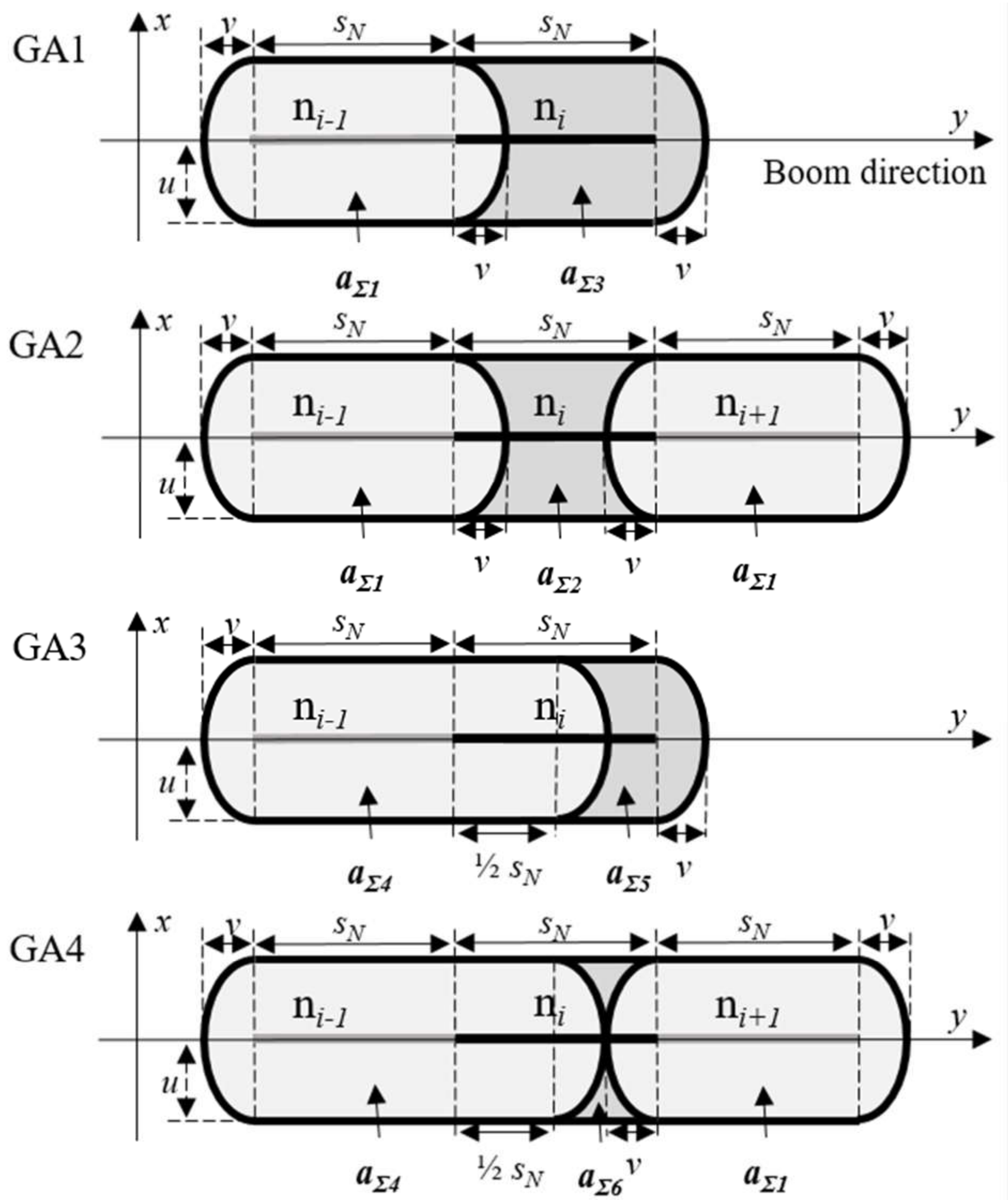

Fig. 4 - Top view of four particular geometric arrangements (GA1 to GA4) of surfaces on which weed patch centres have to be present (dark grey) or absent (light grey) in the neighbouring of an activated detection segment (black segment). *u* and *v* are the semi-major and semi-minor axes of elliptic weed patches, s_N is the nozzle spacing, $a_{\Sigma m}$ (with *m* from 1 to 6) are the areas of the surfaces associated with the detection segments for various geometrical situations.

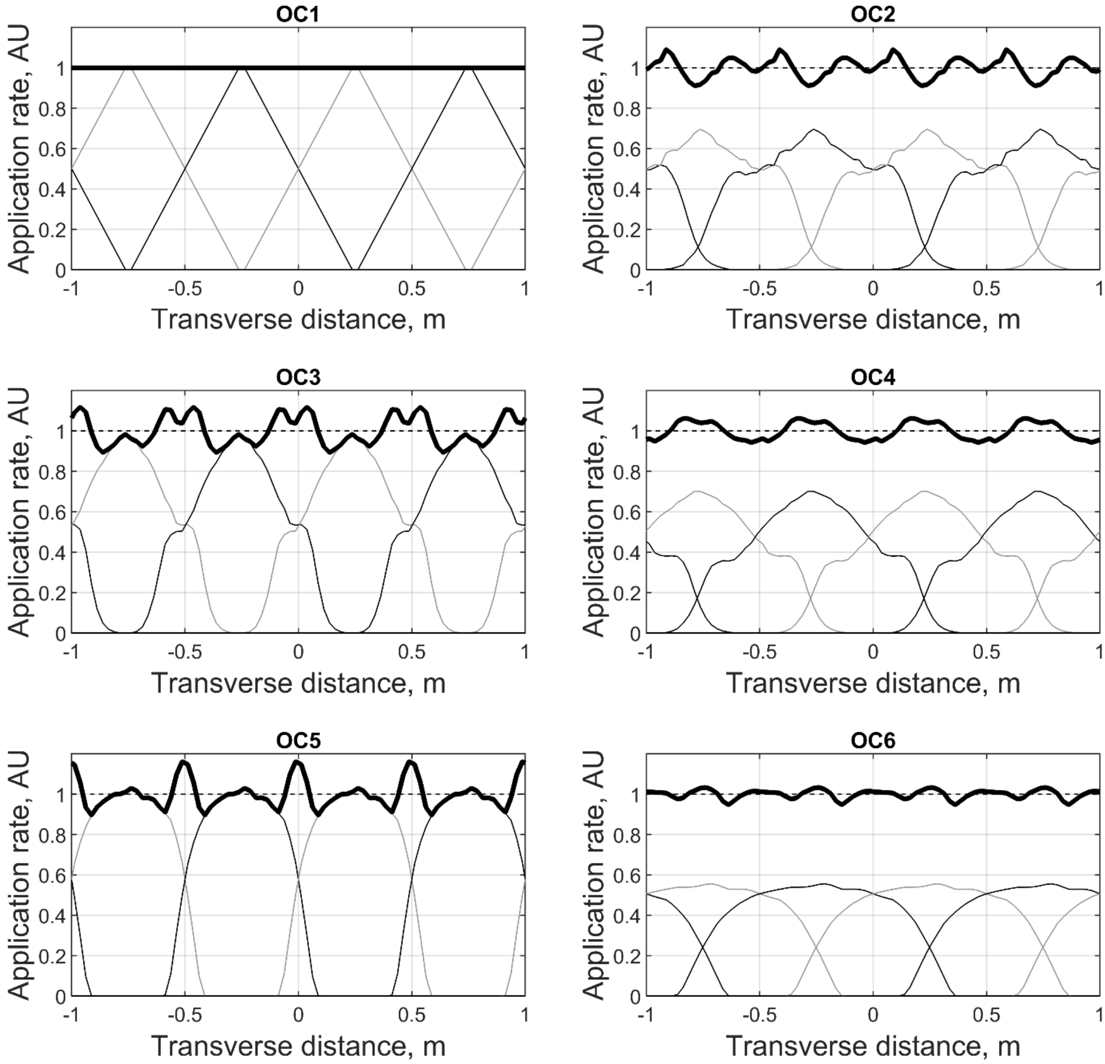

Fig. 5 - Transverse spray patterns of single nozzles (thin lines alternatively grey or black for successive neighbouring nozzles) and global transverse spray patterns resulting from cumulated applications (bold line). The corresponding mean application rate (dotted line) is at the unit value (in Arbitrary Unit (AU)) for all operating conditions (from OC1 to OC6).

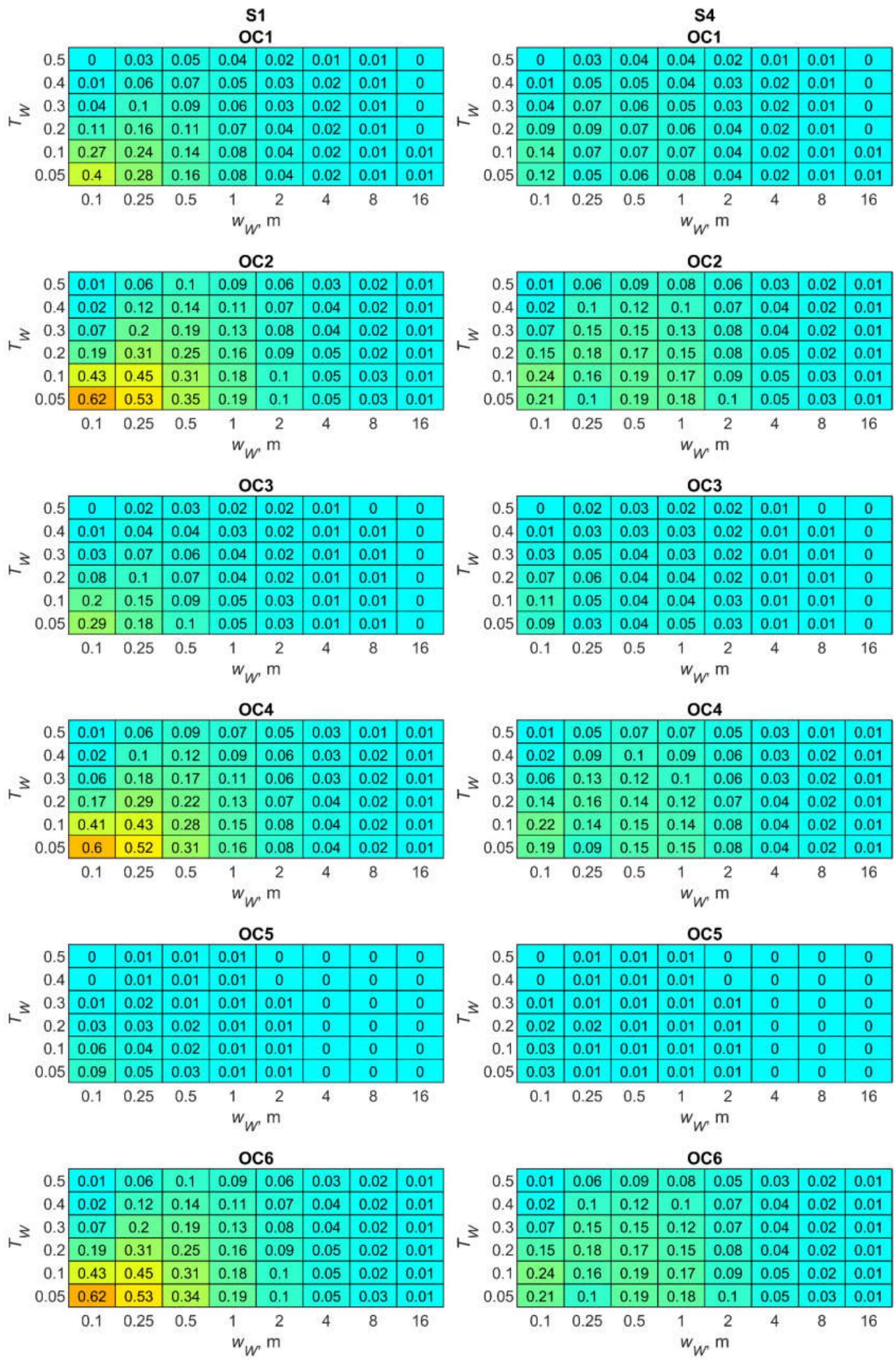

Fig. 6 - Matrices of values of $T_{WA<85\%}$ derived from spraying simulations for strategies S1 (left) and S4 (right), and for all the operating conditions (OC1 to OC6) with respect to weed patch width w_w and weed coverage rate T_w. To improve data readability, the matrix cells are coloured according to values (from blue (value 0) to red (value 1) in the web version or from white (value 0) to grey (value 1) in the printed version of this article).

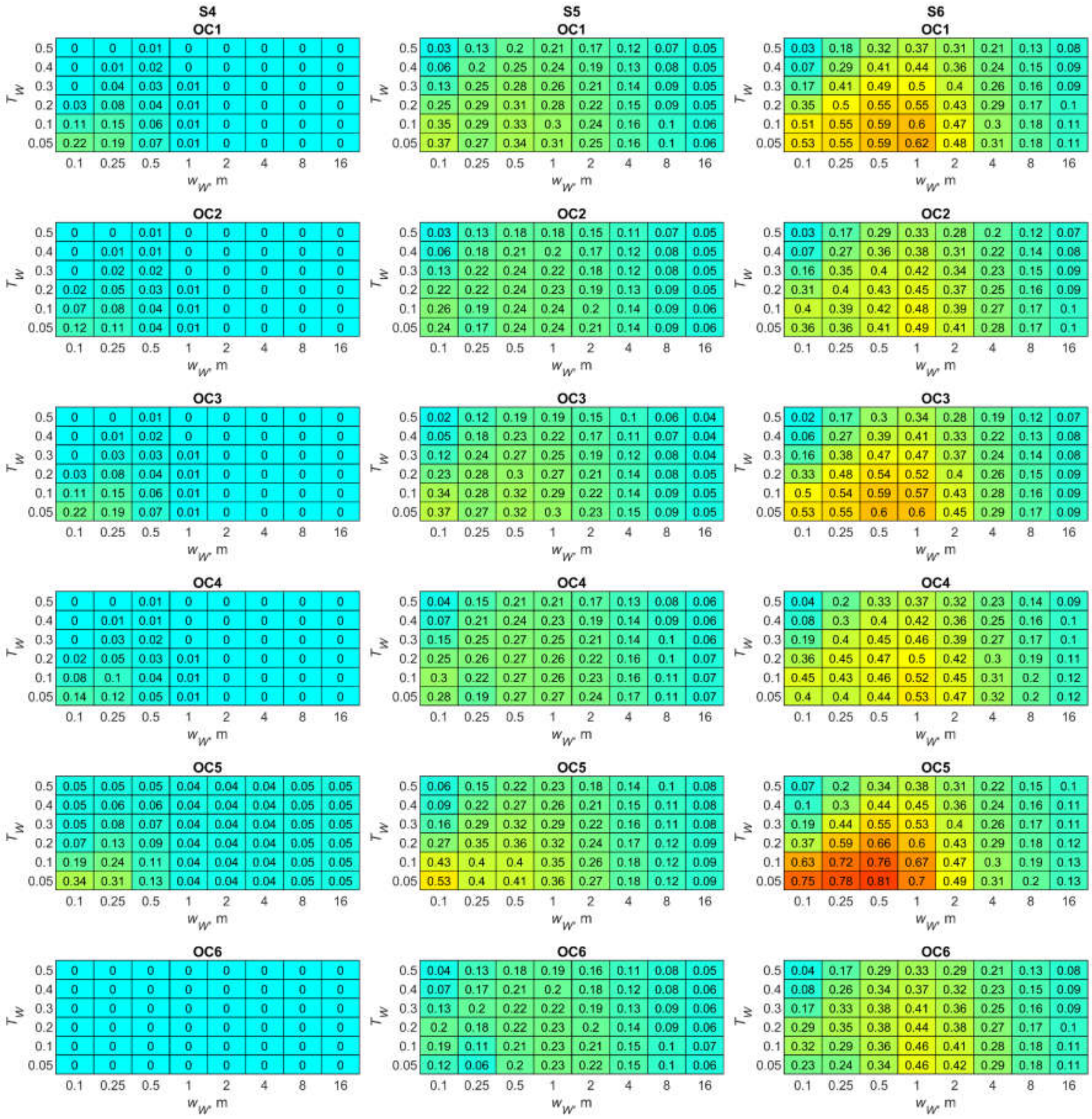

Fig. 7 - Matrices of values of $T_{SA>115\%}$ derived from spraying simulations for strategies S4 (left), S5 (middle), S6 (right) and for all the operating conditions (OC1 to OC6) with respect to weed patch width w_w and weed coverage rate T_w. To improve data readability, the matrix cells are coloured according to values (from blue (value 0) to red (value 1) in the web version or from white (value 0) to grey (value 1) in the printed version of this article).

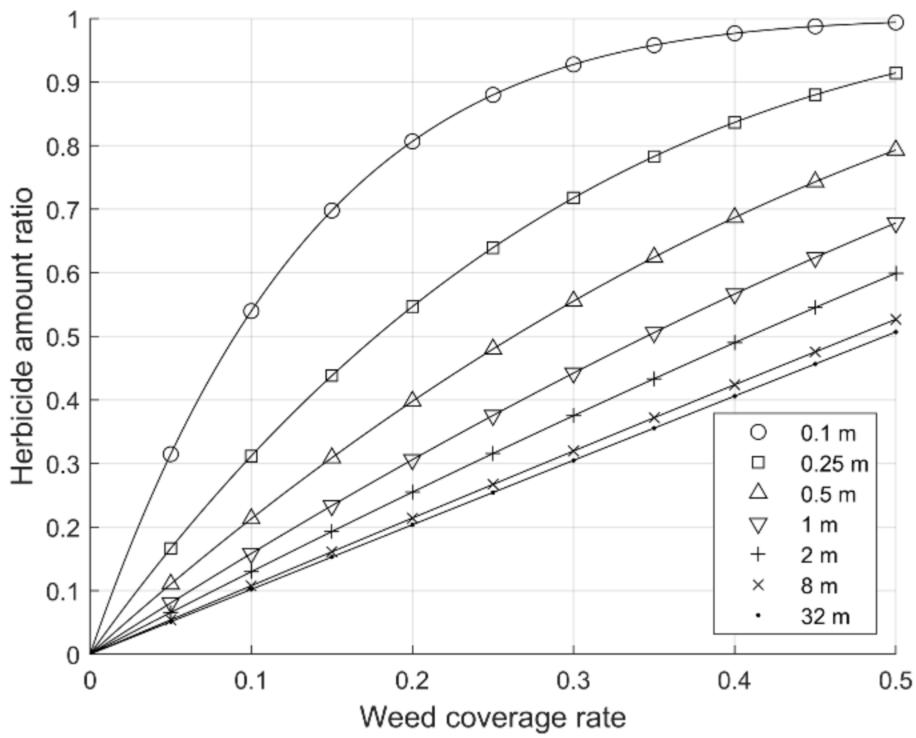

Fig. 8 - Herbicide amount ratio T_Q in the case of the nozzle control strategy S1. The ratio is drawn with respect to the weed coverage rate, for various weed patch widths (from 0.1 to 32 m).

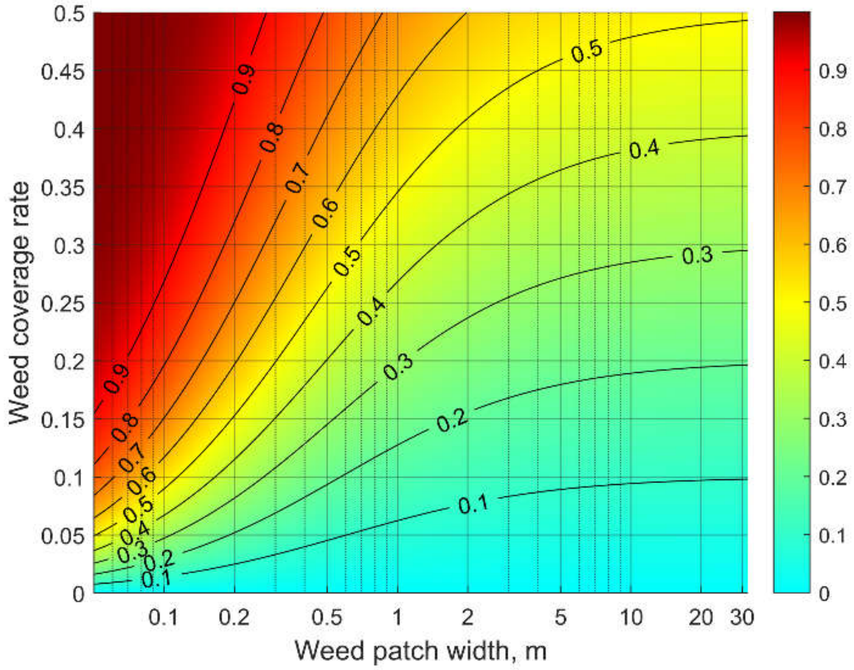

Fig. 9 - Contour graph of the herbicide amount ratio T_Q in the case of the nozzle control strategy S1, with respect to weed patch widths and coverage rates. The colour scale and isolines are representative of T_{QS1}. (For interpretation of the references to colours in this figure legend, the reader is referred to the web version of this article.)

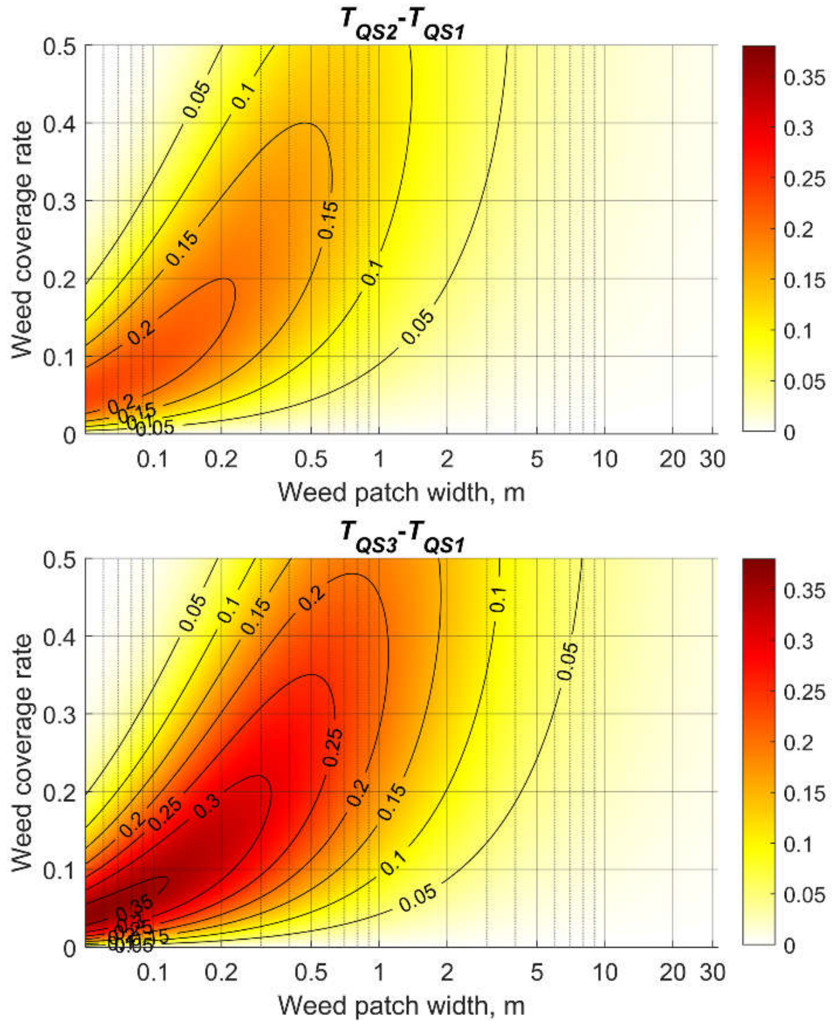

Fig. 10 - Contour graphs of the difference (*i.e.* absolute change) in the herbicide amount ratio between S2 and the reference strategy S1 (top) and between S3 and S1 (bottom). The colour scale and isolines are representative of the differences. (For interpretation of the references to colours in this figure legend, the reader is referred to the web version of this article.)

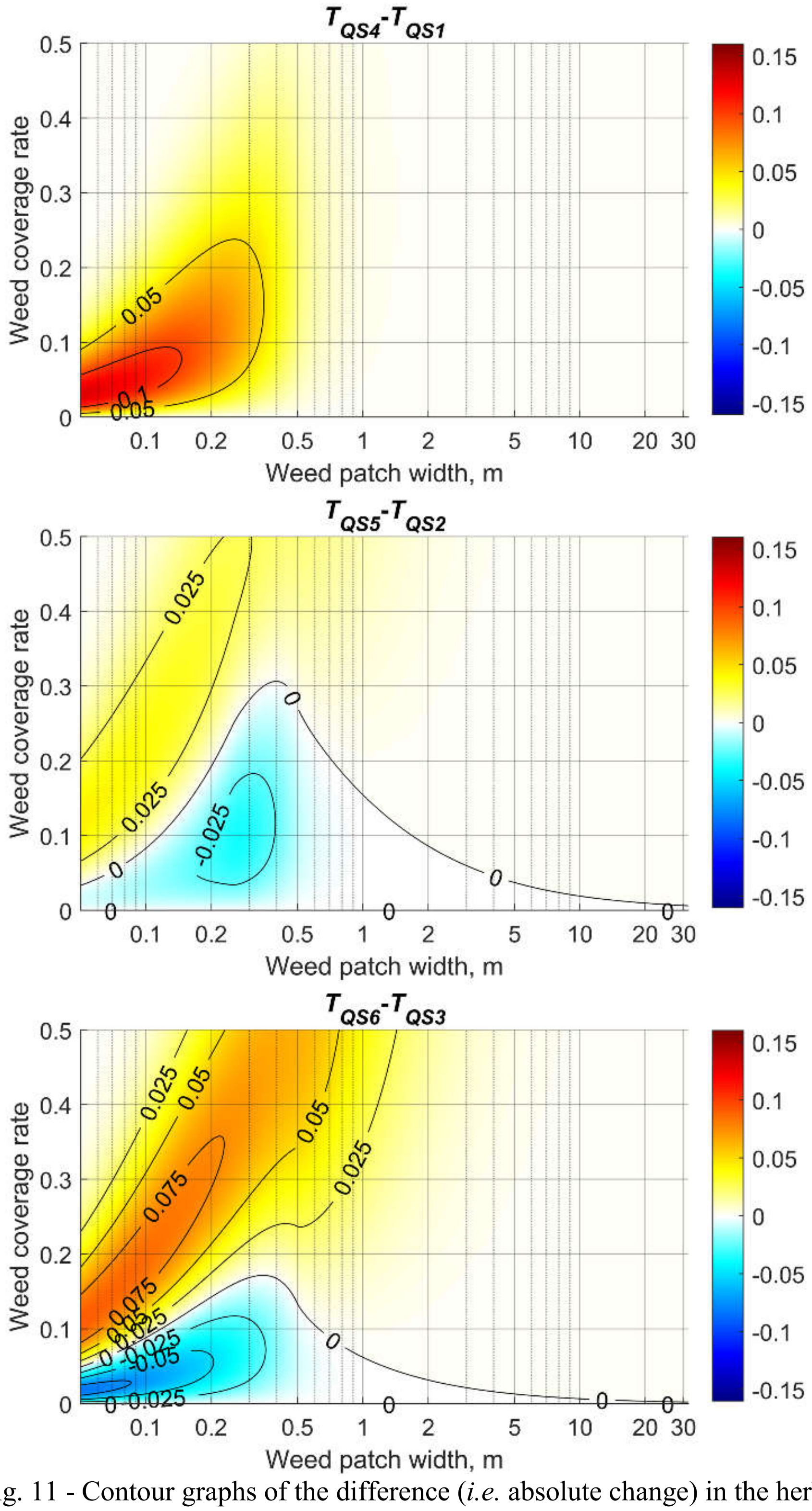

Fig. 11 - Contour graphs of the difference (*i.e.* absolute change) in the herbicide amount ratio between S4 and S1 T_{QS4} - T_{QS1} (top), between S5 and S2 T_{QS5} - T_{QS2} (middle), and between S6 and S3 T_{QS6} - T_{QS3} (bottom). The colour scale and isolines are representative of the differences. (For interpretation of the references to colours in this figure legend, the reader is referred to the web version of this article.)

Table 1
Main characteristics of the six nozzle operating conditions. CV is the coefficient of variation and $\mu_{\delta CVh}$ is the mean change of the CV value when the boom height fluctuates ±0.05 m. The nozzle spacing is 0.5 m for all operating conditions. The spray patterns were developed from data produced by Herbst (2019) for OC2, OC3 and OC4 and by Hassen et al. (2013) for OC5 and OC6.

Operating condition	Nozzle	Shape of the transverse spray pattern	Boom height h_s (m)	CV (%)	$\mu_{\delta CVh}$
OC1	Fictitious	Perfect triangle	0.5	0	2.3
OC2	CVI 110 02	Triangular	0.5	3.6	4.0
OC3	IDK 90 02	Triangular	0.5	6.3	0.6
OC4	IDK 90 02	Triangular	0.7	3.9	2.1
OC5	TPE 80 03	Even	0.35	2.7	13.1
OC6	TPE 80 03	Even	0.65	1.9	3.8

Table 2
Maximal values of $T_{WA<85\%}$ obtained for all weed coverage rates (from 0.05 to 0.5), all patch widths (from 0.1 to 16 m), and for each strategies (S1 to S6) and each operating condition (OC1 to OC6).

Operating condition	Strategy					
	S1	S2	S3	S4	S5	S6
OC1	0.397	0	0	0.144	0	0
OC2	0.624	0.023	0	0.243	0.007	0
OC3	0.293	0	0	0.107	0	0
OC4	0.603	0.008	0	0.218	0.002	0
OC5	0.093	0	0	0.034	0	0
OC6	0.625	0.016	0	0.243	0.005	0